 

https://doi.org/10.1070/QEL17513

# Polyacrylamide-based phantoms of human skin for hyperspectral fluorescence imaging and spectroscopy

V.V. Shupletsov, E.A. Zherebtsov, V.V. Dremin, A.P. Popov,
A.V. Bykov, E.V. Potapova, A.V. Dunaev, I.V. Meglinski

*Abstract.* **Based on the combined use of polymerisable polyacrylamide, collagen and an aqueous solution of Flavin adenine dinucleotide (FAD), we have developed a new technique for fabrication of composite phantoms mimicking fluorescence properties of human skin. A comparative analysis of the absorption and scattering coefficients, refractive indices, as well as fluorescence spectra of phantoms with different concentrations of FAD measured with the combined use of a CCD spectrometer and a hyperspectral camera is presented. To obtain values of scattering coefficients close to those for human skin, zinc oxide (ZnO) nanoparticles are added to the polyacrylamide polymer structure. Variations both in the shape of the spectrum and in the intensity of the fluorescence signal in the phantoms are provided by the changes in the volume fraction of FAD and collagen. It is shown that the model fluorescence spectra are in good agreement with the results of direct human skin measurements *in vivo*.**

***Keywords:*** *optical properties, human skin, phantoms, collagen, flavin adenine dinucleotide, hyperspectral imaging, fluorescence spectroscopy.*

**V.V. Shupletsov, E.V. Potapova, A.V. Dunaev** Research and Development Centre of Biomedical Photonics, State Federal-Funded Educational Institution of Higher Education 'Orel State University named after I.S. Turgenev', Naugorskoe sh. 29, 302020 Orel, Russia; e-mail: valery.shupletsov@bmecenter.ru;
**E.A. Zherebtsov** Research and Development Centre of Biomedical Photonics, State Federal-Funded Educational Institution of Higher Education 'Orel State University named after I.S. Turgenev', Naugorskoe sh. 29, 302020 Orel, Russia; Optoelectronics and Measurement Techniques Unit, University of Oulu, Oulu, 90570, Finland;
**V.V. Dremin** Research and Development Centre of Biomedical Photonics, State Federal-Funded Educational Institution of Higher Education 'Orel State University named after I.S. Turgenev', Naugorskoe sh. 29, 302020 Orel, Russia; College of Engineering and Physical Sciences, Aston University, Birmingham, B4 7ET, UK;
**A.P. Popov** VTT Technical Research Centre of Finland, Oulu, 90571, Finland;
**A.V. Bykov** Optoelectronics and Measurement Techniques Unit, University of Oulu, Oulu, 90570 Finland;
**I.V. Meglinski** College of Engineering and Physical Sciences, Aston University, Birmingham, B4 7ET, UK; National Research Nuclear University MEPhI, Kashirskoe sh. 31, 115409 Moscow, Russia; Optoelectronics and Measurement Techniques Unit, University of Oulu, Oulu, 90570, Finland; Sechenov First Moscow State Medical University, ul. Trubetskaya 8, stroenie 2, 119991 Moscow, Russia

Received 31 December 2020
*Kvantovaya Elektronika* **51** (2) 118–123 (2021)
Translated by M.Yu. Kirillin

## 1. Introduction

Owing to the currently observed steady acceleration of the development of medical diagnostic technologies, the spectrum of optical techniques employed or being introduced in day-to-day clinical practice has significantly widened, including optical coherence tomography (OCT); photoacoustic tomography; optical, Raman, and fluorescence spectroscopy; dynamic light scattering spectroscopy; etc. [1]. Development, calibration measurements, verification and standardisation of an optical diagnostics technique require its comprehensive testing using control biological tissue samples or calibration model phantoms (MPs) with known and quantitatively confirmed optomechanical properties, including structural geometric features and shape. Using MPs as test objects allows for high accuracy calibration of measurement systems, adjustment of measurement technique for obtaining a useful signal/image from a certain depth, and localisation of measured volume, as well as for standardisation of the measurement results obtained by devices from different manufacturers. Note that the standardisation quality significantly depends on the use of materials with controlled optical properties, satisfying the stationarity condition. Since optical the properties of biological tissues vary significantly depending on storage conditions and duration, MPs are highly demanded both at the development stage, and during calibration measurements in the course of the device employment.

Over the past 15–20 years, MPs mimicking optical properties of various biotissues [2] have been developed for a number of diagnostic techniques, such as polarimetry [3], OCT [4], Doppler OCT [5], terahertz spectroscopy [6], fluorescence spectroscopy [7], laser speckle contrast imaging [8], etc. For reproduction of fluorescence parameters in the simplest MPs, aqueous colloidal solutions (for example, intralipid) with the addition of absorbing dyes are used, as well as substances with a pronounced endogenous fluorescence excited in the required in the wavelength range [9–12]. In such MPs, buffer solutions with the required pH value can be used as a matrix material to ensure an environment compatible with the natural structure of organic molecules mimicking certain properties of a living organism [13, 14]. When developing MPs mimicking a vascular capillary bed, different personal porous structures are used allowing one to achieve the best similarity of structural and geometric features of a test object under development for verification of optical measurements [15]. To imitate soft tissues, MPs with hybrid structure are used, such as gel–wax or mineral–oil material based ones [16]. MPs containing dimethylformamide as a solvent and protopor-

phyrin IX as a fluorophore were proposed, mimicking the fluorescence parameters of tumour tissues [11].

To develop an MP with the required dimensions, geometric shape and the presence of a heterogeneity, the use of plastic layers with specified absorbing, scattering and fluorescent properties is typical. In their manufacturing, such materials like carrageenan, polysaccharide, agar, agarose, polyvinyl alcohol, polyurethane, silicone, as well as elastomeric (rubber-like) substances are used [17, 18]. Produced test objects satisfy the stationarity requirement and allow for reproduction of a multi-layer tissue structure with the specified properties of each individual layer [19]. The use of plastic materials allows designing shapes with hollow areas and solid inclusions, for example, to imitate blood vessels [20] and other macroinhomogeneities within biotissues [21]. The use of a silicone base mixed with glycerin allows designing MPs of biotissues that have their own scattering, which significantly improves the stability of obtained properties [22], while the use of a plastic matrix base allows the fabrication of composite MPs with liquid fragments, for example from alcohol-soluble nigrosine and bovine hemin [23], or flexible mesh structures from polyamide [24].

MPs of skin and brain based on polyvinyl chloride and siliconethat have demonstrated their effectiveness and stability when verifying measurements by various techniques, including hyperspectral imaging, OCT, laser speckle contrast imaging, etc., which were previously described in [19, 20, 22, 25–28]. However, such MPs have significant limitations in mimicking fluorescent properties of biotissues. The conditions of the polymerisation processes (increased temperature, use of chemically active polymerising substances) lead to destruction or significant variation in the properties of fluorescence dyes, especially in the properties of such endogenous fluorescent substances as nicotinamide adenine nucleotide (NADH) and flavin adenine nucleotide (FAD).

This work presents for the first time a manufacturing technique and main optical properties of a new human skin MP type based on polymerisable polyacrylamide (PAA), collagen and aqueous solution of FAD. PAA is an optically transparent elastic material with a good temporal photostability, which is actively used in biomedical practice. To simulate the base level of skin connective tissue fluorescence, the collagen contained in gelatin was used. Hard gelatinous MPs were used to mimic normal and dysplasic biotissue states in diagnostics with fluorescent techniques [29, 30]. For the developed approach, moderate polymerisation modes are typical, which do not affect FAD fluorescence. In order to design a denser elastic structure, not subject to mold, the PAA gel was used as a bounding material with stable thermal and chemical properties [31].

An important feature of the developed fluorescent MPs is the lack of own pronounced fluorescence of PAA in UV and visible ranges. An aqueous FAD solution, which is one of the main skin fluorophores upon excitation at a wavelength of 450 nm was used as a fluorophore. In the human body, FAD plays a key role in processes of cellular respiration and cell death, as well as in the continuous utilisation of endogenous catecholamines (such as dopamine, adrenaline, norepinephrine, etc.), being a co-factor of two known varieties of FAD-dependent monoamine oxidases primarily responsible for the processes of deamination in the majority of organism's cells. Alterations in the FAD fluorescence parameters (intensity, spectrum shape, and lifetime) are essential diagnostic signs of a pathology development [32]. For example, previously conducted clinical studies show that alterations in FAD fluorescence correlate with oncological processes [33–35].

Thus, the aim of this work is the development of an elastic MP mimicking FAD fluorescence in the skin for calibration measurements and verification of endogenous fluorescence registration systems.

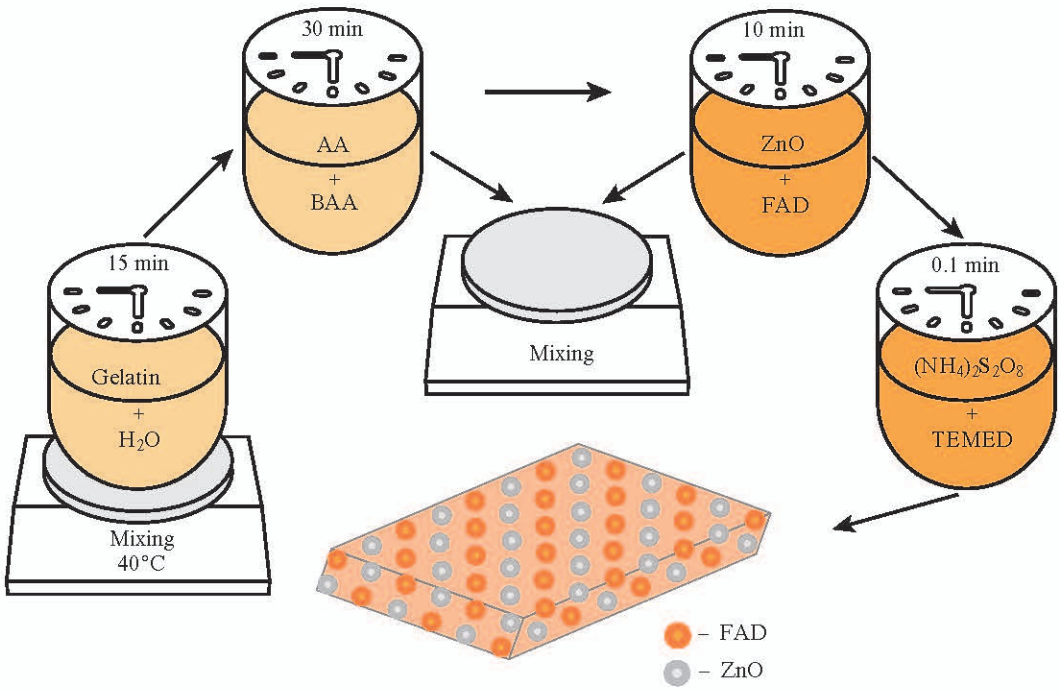


**Figure 1.** Sequences of the main stages of fabrication of human skin MPs based on collagen, PAA gel, zinc oxide and aqueous FAD solution, as well as the appearance of the plastic composite base.

## 2. Materials and methods

*Designing a model skin phantom.* Preliminary preparation of an elastic matrix base of human skin MPs was carried out by mixing and homogenising powdered gelatin (0.2 g) with 20 mL of distilled water until a homogeneous structure is obtained upon heating to 40 °C for 15 min. Subsequent homogenisation of the obtained solution was carried out by mixing acrylamide (AA) (6 g) and bisacrylamide (BAA) (0.16 g) at room temperature for 15 min. To reproduce scattering properties, zinc oxide (ZnO) in the amount of 0.03 g was added to the manufactured polymer structure [36, 37].

To reproduce the fluorescence properties, FAD (which concentration normally varies in human body from several units up to several tens of μmoles per 100 g of tissue [38]) was added to the obtained mixture, and they were mixed for 10 min. Five skin MPs were fabricated: without FAD and with FAD concentrations of 5, 15, 20, and 25 μmoles per 100 g of material.

Subsequent polymerisation until elastic light-scattering structure was performed by adding 15 μL of ammonium persulfate [$(NH_4)_2S_2O_8$] and 2.4 μL of tetramethylethylenediamine (TEMED).

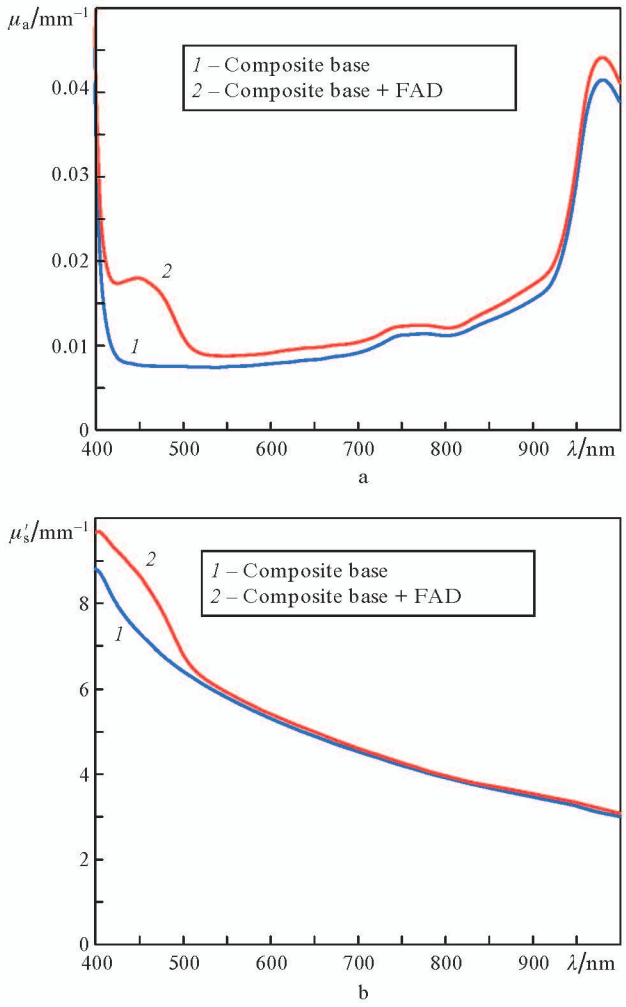


**Figure 2.** Spectral dependences of (a) absorption coefficients and reduced (b) scattering coefficients of the fabricated composite base without FAD and with the addition of 15 μM of FAD.

Diffuse reflectance, diffuse and collimated transmittance of the manufactured plastic composite base (Fig. 1), as well as the base with the addition of 15 μM FAD were measured with a spectrophotometer equipped with an integrating sphere (Gooch & Housego, USA) [39]. Absorption coefficient ($\mu_a$) and reduced scattering coefficient ($\mu_s'$) were calculated by the inverse add-d-oubling technique in the range 400–1000 nm (Fig. 2).

The absorption spectra clearly show water absorption bands (760 and 975 nm) and a FAD absorption band (450 nm). Since the main aim of this work is mimicking fluorescence, no additional absorption components aiming to achieve absorption equivalent to that of skin tissues were added to PAA based bounding matrix in course of MP manufacturing. Refractive indices $\mu_s$ of MPs were measured using an Abbe multiwave refractometer (Atago, Japan) at different wavelengths: $n$ = 1.358 (450 nm), 1.350 (589 nm), 1.348 (632 nm), and 1.343 (930 nm).

*Experimental equipment.* Fluorescence parameters were measured using a setup including a hyperspectral camera and a CCD spectrometer (Fig. 3). Radiation from a M450LP1 LED at a wavelength of 450 nm (Thorlabs, USA) passes through a bandpass filter MF445-45 (Thorlabs). Transmitted radiation band goes to a dichroic filter MD416 (Thorlabs) and is then directed to a skin MP for FAD fluorescence excitation. The back-reflected LED radiation is removed from the light flux with a dichroic filter and a light filter FELH0500 with a cut-off wavelength of 500 nm (Thorlabs). Remaining sample fluorescence emission is recorded by a Specim hyperspectral camera (Spectral Imaging Ltd., Finland) in the spectral range of 400–1000 nm. In the fluorescence spectroscopy channel, the spectra are registered with a CCD spectrometer

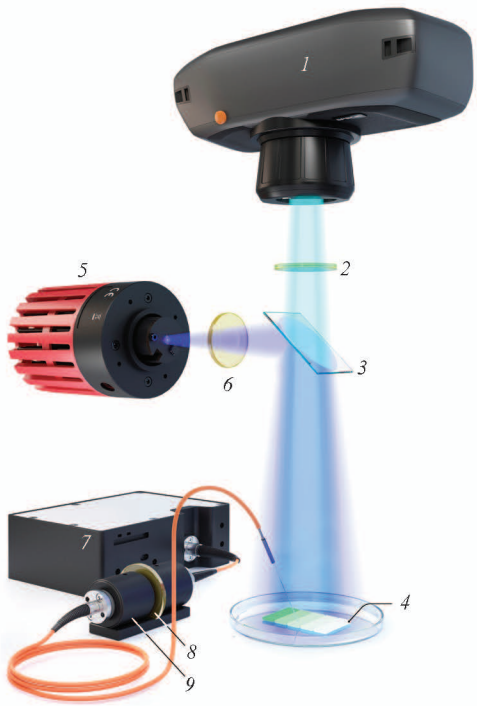


**Figure 3.** Setup for hyperspectral fluorescence imaging and fluorescence spectroscopy: (*1*) hyperspectral camera; (*2*, *9*) long-wavelength emission filter; (*3*) dichroic filter; (*4*) test object; (*5*) LED source; (*6*) bandpass filter; (*7*) CCD spectrometer; (*8*) filter holder.

FLAME-T-VIS-NIR-ES (Ocean Optics, USA) in the spectral range of 350–820 nm using optical fibre.

## 3. Results and discussion

The acquired hyperspectral fluorescence images of five skin MPs with different concentration of FAD are shown in Fig. 4a. The images were registered with a camera exposition time of 500 ms and an average irradiance of 0.5 mW cm$^{-2}$. For further analysis the fluorescence intensity values were averaged within the region of interest (ROI) boundaries, similar to those marked with a square in Fig. 4a. For comparison of fluorescence properties of elastic MPs with a real biological object, fluorescence images of human finger skin and forearm

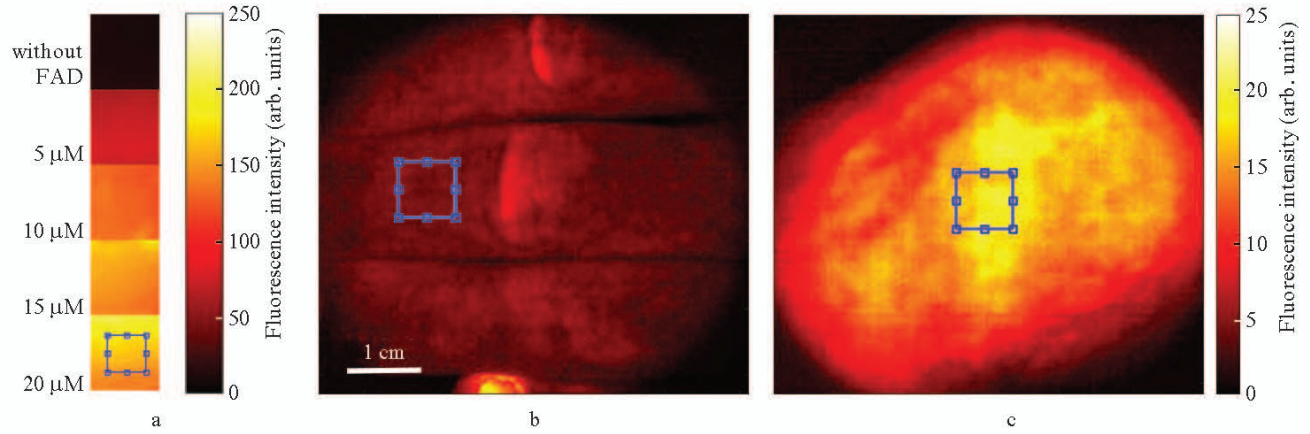


**Figure 4.** Fluorescence images of (a) MPs, (b) finger skin *in vivo*, and (c) forearm skin *in vivo*, obtained using a hyperspectral camera at a wavelength of 530 nm.

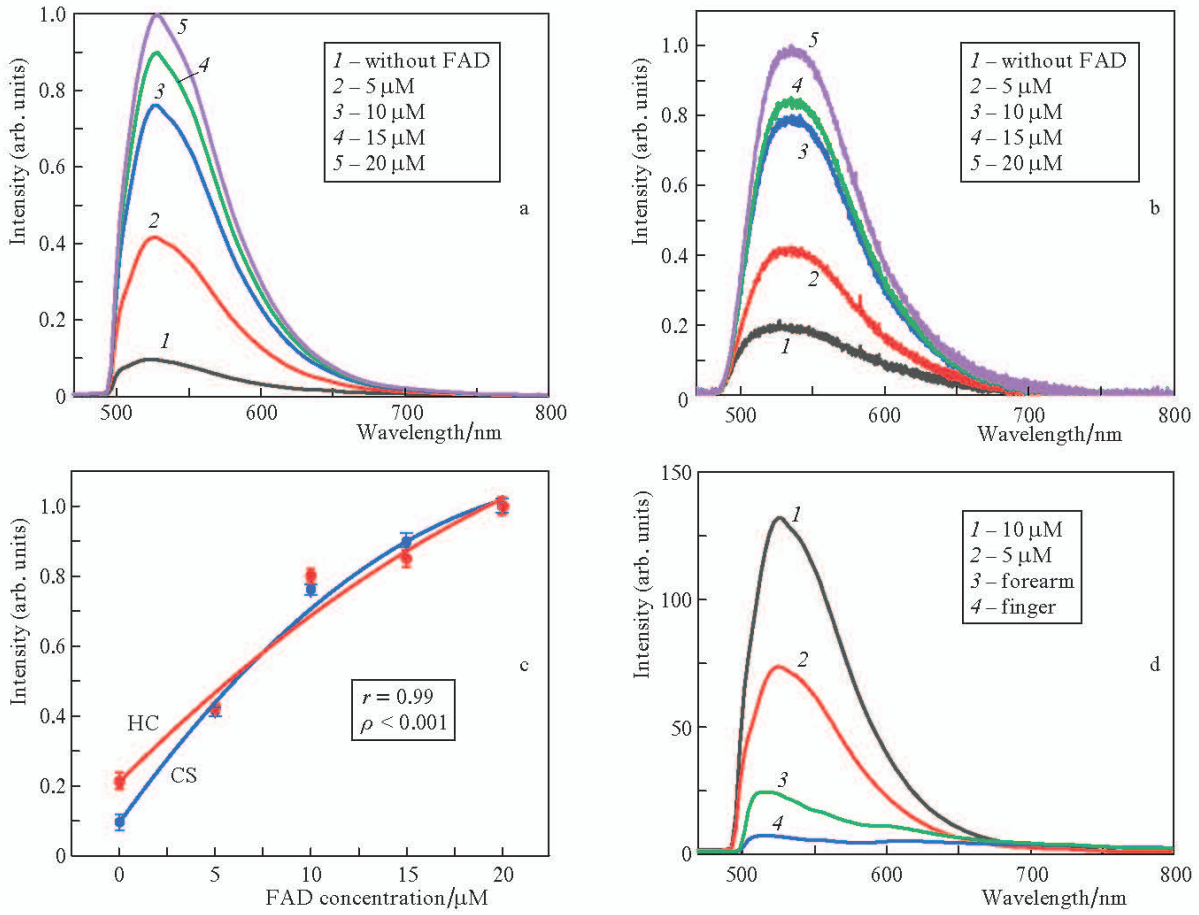


**Figure 5.** (a, b) Fluorescence spectra of skin MPs obtained using (a) a hyperspectral camera and (b) a CCD spectrometer, (c) dependences of maximum MP fluorescence intensity vs. FAD concentration and (d) spectra of maximum MP fluorescence for two FAD concentrations and maximum fluorescence of the finger and forearm skin obtained with a hyperspectral camera; (HC) hyperspectral camera, (CS) CCD spectrometer.

skin of a healthy volunteer were acquired (Figs 4b and 4c). Data from the selected ROIs after spatial averaging were used for construction and analysis of fluorescence intensity spectra.

The maximum intensity values measured with a CCD spectrometer were averaged over three spectra for each MP and compared with the data obtained using a hyperspectral camera.

Figures 5a – 5c show normalised fluorescence spectra and curves for dependence of the maximum MP fluorescence intensity versus FAD concentration obtained using hyperspectral imaging and CCD spectroscopy. Fluorescence spectra of MPs and skin (Fig. 5d) were normalised to the maximum fluorescence value for a concentration of 25 μM and forearm fluorescence intensity, respectively. FAD fluorescence intensity registered in the channel of fluorescence imaging with a hyperspectral camera varies in proportion to fluorophore concentration, which was also confirmed by CCD spectrometer measurements (Fig. 5c). Moreover, the highest intensity variation rate with a FAD concentration change is observed in the range of 5 – 10 μM, which is of greatest interest in mimicking healthy tissue properties. The obtained fluorescence intensity values for MPs have a high correlation with FAD concentration (Pearson's correlation coefficient between measurements with two techniques is $r = 0.99$, $p < 0.001$). Variation of the fluorescence intensity signal to the fluorophore concentration ratio is a nonlinear function due to absorption of the excitation radiation by a fluorophore and variations in the useful MP/tissue volume, the signal from which is measured. In the general case, determination of this dependence is a nontrivial problem, the final decision of which is affected by fluorophore concentration, object absorbing and scattering properties, as well as the parameters of the detection system. Spectra of manufactured MPs and spectra of human skin have similar fluorescence peaks corresponding to the FAD spectrum ($\lambda_{max} \approx 530 - 540$ nm) under excitation with blue light (450 nm). However, the shape of the skin fluorescence spectra, as well as the general signal intensity level are different from those for MPs, which is explained by the effect of blood on fluorescence absorption in skin. Moreover, the presented phantoms can be modified to account for absorbing properties at no significant cost.

A higher initial fluorescence level (Fig. 5c) obtained during measurements with a fibre-optic CCD spectrometer without FAD is explained by the contribution of radiation to the measured signal from a greater depth of the MP probe volume. A significant difference in skin fluorescence intensity for finger and forearm (Fig. 5d) is due to a sufficiently large number of capillaries and arteriovenular anastomoses in hand palm skin [40], which significantly affects fluorescence signal absorption.

## 4. Conclusions

The paper presents a technique for fabricating a new type human skin MP based on PAA, collagen, zinc oxide, and FAD aqueous solution. The main advantage of the developed MPs is that the conditions for PAA polymerisation do not affect FAD fluorescence properties in final phantoms. At the same time, fabricated polymeric MPs with confirmed scattering and fluorescence properties allow reproduction of skin fluorescence spectra in the specified wavelength range with a sufficiently high accuracy. The developed elastic MP matrix satisfies the stationarity condition required for calibration measurements. Manufactured forms should be stored at a temperature of 4 °C and air humidity at a level of 90 % – 95 %. Application of the developed MP manufacturing technology will allow testing, standardising and calibrating systems for fluorescence imaging, as well as instruments for fluorescence spectroscopy, coupled with fibre-optic detection of optical radiation. For improvement and further development of the presented technique a design of MPs is planned containing fluorophores that are endogenous markers of neoplastic changes in tissues, such as NADH and protoporphyrin IX.

***Acknowledgements.*** The work was supported by the Russian Foundation for Basic Research (Project Nos 18-02-00669 and 19-72-30012). A.D. and I.M. thank the Academy of Finland for the support of Projects Nos 326204 and 325097. V.D. acknowledges personal support from the European Union's Horizon 2020 research and innovation programme under the Marie Składowska-Curie Grant Agreement No. 839888. V.Sh. and E.Zh. thank Russian Science Foundation (Grant No. 20-75-00123, development of the composition of samples). The authors are also grateful to Timo Hyvarinen and Katja Lefevre (Spectral Imaging Ltd., Finland) for the equipment provided.

## References

1. Tuchin V.V. *Handbook of Optical Biomedical Diagnostics*: *Vol. 1. Light-Tissue Interaction* (Bellingham, Washington: SPIE Press, 2016).
2. Pogue B.W., Patterson M.S. *J. Biomed. Opt.*, **11**, 041102 (2006).
3. Chue-Sang J., Gonzale M., Pierre A., Laughrey M., Saytashev I., Novikova T., Ramella-Roman J. *J. Biomed. Opt.*, **24**, 030901 (2019).
4. Lamouche G., Kennedy B.F., Kennedy K.M., Bisaillon C.E., Curatolo A., Campbell G., Sampson D.D. *Biomed. Opt. Express*, **3**, 1381 (2012).
5. Bonesi M., Churmakov D.Y., Meglinski I. *Measur. Sci. Technol.*, **18**, 3279 (2007).
6. Zhang T., Nazarov R., Popov A.P., Demchenko P.S., Bykov A.V., Grigorev R.O., Kuzikova A.N., Soboleva V., Zykov D.V., Meglinski I., Khodzitskiy M.K. *J. Biomed. Opt.*, **25**, 123002 (2020).
7. Leh B., Siebert R., Hamzeh H., Menard L., Duval M. A., Charon Y., Abi-Haidar D. *J. Biomed. Opt.*, **17**, 108001 (2012).
8. Sdobnov A. A., Bykov A.G., Molodij G., Kalchenko V., Jarvinen T., Popov A.K., Kordas K.I., Meglinski I. *J. Phys. D: Appl. Phys.*, **51**, 155401 (2018).
9. Potapova E.V., Dremin V.V., Zherebtsov E.A., Podmasteryev K.V., Dunaev A.V. *Fund. Prikl. Probl. Tekh. Tekhnol.*, **332**, 105 (2018) (in Russian).
10. Loginova D.A., Sergeeva E.A., Krainov A.D., Agrba P.D., Kirillin M.Yu. *Quantum Electron.*, **46**, 528 (2016) [*Kvantovaya Elektron.*, **46**, 528 (2016)].
11. Lu H., Floris F., Rensing M., Andersson-Engels S. *Materials*, **13**, 2105 (2020).
12. Luthjens L.H., Yao T., Warman J.M. *Polymers*, **10**, 1195 (2018).
13. Fajardo C., Solarte E. *J. Phys.: Conf. Ser.*, **1547**, 012026 (2020).
14. Beaulieu E., Laurence A., Birlea M., Sheehy G., Angulo-Rodriguez L., Latour M., Leblond F. *Biomed. Opt. Express*, **11**, 2052 (2020).
15. Jayarathna S., Ahmed M.F., Cho S.H. *Molec. Med. Engineering.*, **22**, 4 (2019).
16. Xie Y., Maneas E., Islam S., Peveler W., Shapey J., Xia W., Vercauteren T. *Proc. SPIE*, **10862**, 108621F (2019).
17. Anastasopoulou M., Gorpas D., Koch M., Garcia-Allende P.B., Klemm U., Karlas A., Ntziachristos V. *Proc. SPIE*, **10411**, 104110J (2017).
18. Ahmad M.S., Suardi N., Shukri A., Mohammad H., Oglat A.A., Alarab A., Makhamrah O. *J. Med. Ultrasound*, **28**, 7 (2020).
19. Wróbel M.S., Popov A.P., Bykov A.V., Kinnunen M., Jędrzejewska-Szczerska M., Tuchin V.V. *J. Innovat. Opt. Health Sci.*, **8**, 1541005 (2015).

20. Zherebtsov E., Dremin V., Popov A., Doronin A., Kurakina D., Kirillin M., Bykov A. *Biomed. Opt. Express*, **10**, 3545 (2019).
21. Daly M.J., Fleisig J., Chan H., Ferrari M., Douglas C., Wilson B.C., Irish J.C. *Proc. SPIE*, **11222**, 112220E (2020).
22. Wróbel M.S., Popov A.P., Bykov A.V., Tuchin V.V., Jędrzejewska-Szczerska M. *Biomed. Opt. Express*, **7**, 2088 (2016).
23. Gorpas D., Koch M., Anastasopoulou M., Bozhko D., Klemm U., Nieberler M., Ntziachristos V. *IEEE Transact. Biomed. Eng.*, **67**, 185 (2019).
24. Liu X., Wang R., Ma J., Zhang J., Jiang P., Wang Y., Tu G. *J. Mater. Sci. Technol.*, **11**, 9 (2020).
25. Bykov A.V., Popov A.P., Kinnunen M., Prykäri T., Priezzhev A.V., Myllylä R. *Proc. SPIE*, **7376**, 73760F (2010).
26. Bykov A.V., Popov A.P., Priezzhev A.V., Myllylä R. *Proc. SPIE*, **8091**, 80911R (2011).
27. Sieryi O., Popov A., Kalchenko V., Bykov A., Meglinski I. *Proc. SPIE*, **11363**, 1136312 (2020).
28. Bykov A., Zherebtsov E., Dremin V., Popov A., Doronin A., Meglinski I. *Computat. Opt. Sens. Imag.*, **3**, CW1A (2019).
29. Shupletsov V., Kandurova K., Dremin V., Potapova E., Apanaykin M., Legchenko U., Dunaev A. *J. Biomed. Photon. Eng.*, **6**, 010303 (2020).
30. Shupletsov V., Kandurova K., Stavtsev D., Stolbov A., Potapova E., Dremin D., Vinokurov A., Podmasteryev K., Dunaev A. *Proc. SPIE*, **11457**, 1145708 (2020).
31. Anugrah M.A., Suryani S., Ilyas S., Mutmainna I., Fahri A.N., Tahir D. *Radiat. Phys. Chem.*, **173**, 108878 (2020).
32. Shukla S., Singh P., Pandey P.K., Pradhan A. *Proc. SPIE*, **11363**, 113631L (2020).
33. Wu Y., Xi P., Qu J.Y., Cheung T.H., Yu M.Y. *Opt. Express*, **13**, 382 (2005).
34. Lukina M.M., Shirmanova M.V., Sergeeva T.F., Zagaynova E.V. *Modern Technol. Med.*, **8**, 113 (2016).
35. Pavlova I., Sokolov K., Drezek R., Malpica A., Follen M., Richards-Kortum R. *Photochem. Photobiol.*, **77**, 550 (2003).
36. Krasnikov I.V., Seteikin A.Yu., Popov A.P. *Opt. Spectrosc.*, **118**, 668 (2015) [*Opt. Spectrosk.*, **118**, 698 (2015)].
37. Wróbel M.S., Popov A.P., Bykov A.V., Kinnunen M., Jędrzejewska-Szczerska M., Tuchin V.V. *J. Biomed. Opt.*, **20**, 045004 (2015).
38. Moffitt T.P., Chen Y.C., Prahl S.A. *J. Biomed. Opt.*, **11**, 041103 (2006).
39. Aliverti A., Curti B., Vanoni M.A. *Meth. Molec. Biol.*, **131**, 9 (1999).
40. Guyton A.C. *Textbook of Medical Physiology* (Amsterdam: Elsevier, 2015).